Ruling out pyridine dinucleotides as true TRPM2 channel activators reveals novel direct agonist ADP-ribose-2′-phosphate

Balázs Tóth,[1,2] Iordan Iordanov,[1,2] and László Csanády[1,2]

[1]Department of Medical Biochemistry and [2]MTA-SE Ion Channel Research Group, Semmelweis University, Budapest H-1094, Hungary

Transient receptor potential melastatin 2 (TRPM2), a Ca^{2+}-permeable cation channel implicated in postischemic neuronal cell death, leukocyte activation, and insulin secretion, is activated by intracellular ADP ribose (ADPR). In addition, the pyridine dinucleotides nicotinamide-adenine-dinucleotide (NAD), nicotinic acid–adenine-dinucleotide (NAAD), and NAAD-2′-phosphate (NAADP) have been shown to activate TRPM2, or to enhance its activation by ADPR, when dialyzed into cells. The precise subset of nucleotides that act directly on the TRPM2 protein, however, is unknown. Here, we use a heterologously expressed, affinity-purified–specific ADPR hydrolase to purify commercial preparations of pyridine dinucleotides from substantial contaminations by ADPR or ADPR-2′-phosphate (ADPRP). Direct application of purified NAD, NAAD, or NAADP to the cytosolic face of TRPM2 channels in inside-out patches demonstrated that none of them stimulates gating, or affects channel activation by ADPR, indicating that none of these dinucleotides directly binds to TRPM2. Instead, our experiments identify for the first time ADPRP as a true direct TRPM2 agonist of potential biological interest.

The Journal of General Physiology

INTRODUCTION

Transient receptor potential melastatin 2 (TRPM2) is a Ca^{2+}-permeable cation channel (Perraud et al., 2001; Sano et al., 2001), which is activated under conditions of oxidative stress (Hara et al., 2002). It is expressed in the spleen, bone marrow, leukocytes, pancreatic β cells, and most abundantly in the brain (Nagamine et al., 1998; Perraud et al., 2001; Togashi et al., 2006), and plays central roles in chemokine-induced phagocyte activation (Yamamoto et al., 2008), insulin secretion (Uchida et al., 2011), neuronal apoptosis after cerebral stroke (Hara et al., 2002; Kaneko et al., 2006; Olah et al., 2009), as well as in the development of several neurodegenerative diseases (Fonfria et al., 2005; Hermosura et al., 2008).

TRPM2 channels are homotetramers. In addition to a transmembrane domain with a topology conserved among all TRP family ion channels and a large N-terminal cytosolic region of unknown function, specific to members of the TRPM subfamily, TRPM2 contains a unique C-terminal NUDT9 homology (NUDT9H) domain, which shares ∼40% sequence identity with the soluble mitochondrial enzyme NUDT9 (Perraud et al., 2003a). The latter is a specific ADP ribose (ADPR) pyrophosphatase (ADPRase), which cleaves ADPR into AMP and ribose-5-phosphate (Perraud et al., 2003b). Prompted by this sequence homology, TRPM2 channels were discovered to be activated by binding, to the NUDT9H domain, of ADPR (Perraud et al., 2001; Sano et al., 2001) released from mitochondria under conditions of oxidative stress (Perraud et al., 2005).

The biophysical mechanism of TRPM2 channel gating is complex and requires the simultaneous presence of micromolar cytosolic Ca^{2+} and ADPR (McHugh et al., 2003; Csanády and Törocsik, 2009); some phosphatidylinositol 4,5-bisphosphate (PIP_2) in the inner membrane leaflet is also essential because after complete PIP_2 depletion, TRPM2 channels can be opened only in the presence of millimolar Ca^{2+} (Tóth and Csanády, 2012). The binding sites for activating Ca^{2+} are unknown but must be located very near the cytosolic pore entrance because they are kept saturated by extracellular Ca^{2+} ions entering through the open channel pore (Csanády and Törocsik, 2009). However, whereas in intact cells TRPM2 channels supply themselves with the necessary Ca^{2+}, in excised inside-out patches under continuous superfusion the high local Ca^{2+} concentration required for TRPM2 gating can be secured only by inclusion of high micromolar Ca^{2+} in the bath solution: even millimolar ADPR only marginally activates TRPM2 channels when (local) intracellular Ca^{2+} concentration

Correspondence to László Csanády: csanay.laszlo@med.semmelweis-univ.hu

Abbreviations used in this paper: ADPR, ADP ribose; ADPRase, ADPR pyrophosphatase; ADPRP, ADPR-2′-phosphate; AMPP, AMP-2′-phosphate; cADPR, cyclic ADPR; NAAD, nicotinic acid–adenine-dinucleotide; NAADP, NAAD-phosphate; NAD, nicotinamide-adenine-dinucleotide; NUDT9H, NUDT9 homology; PIP_2, phosphatidylinositol 4,5-bisphosphate; TLC, thin-layer chromatography; TRPM2, transient receptor potential melastatin 2.

© 2015 Tóth et al. This article is distributed under the terms of an Attribution–Noncommercial–Share Alike–No Mirror Sites license for the first six months after the publication date (see http://www.rupress.org/terms). After six months it is available under a Creative Commons License (Attribution–Noncommercial–Share Alike 3.0 Unported license, as described at http://creativecommons.org/licenses/by-nc-sa/3.0/).

The Rockefeller University Press $30.00
J. Gen. Physiol. Vol. 145 No. 5 419–430
www.jgp.org/cgi/doi/10.1085/jgp.201511377

Downloaded from http://rupress.org/jgp/article-pdf/145/5/419/1794700/jgp_201511377.pdf by guest on 07 February 2026

is lowered to 1 µM (Tóth and Csanády, 2010). In the presence of Ca^{2+}, bursts of channel openings (Csanády and Törocsik, 2009) are elicited by mere binding of ADPR: a low turnover ADPRase activity reported for the isolated NUDT9H domain (Perraud et al., 2001, 2003b) was shown not to be coupled to channel gating (Tóth et al., 2014). Rapid irreversible inactivation of WT TRPM2 channels in inside-out patches is caused by a conformational change of the selectivity filter and can be overcome by a triple pore substitution: the "T5L" TRPM2 variant allows long steady-state recordings while preserving all features of WT TRPM2 gating (Tóth and Csanády, 2012).

Additional modulators of TRPM2 channel activity were identified in numerous studies. In particular, hydrogen peroxide (H_2O_2; Wehage et al., 2002) and various adenine nucleotides including cyclic ADPR (cADPR; Beck et al., 2006; Lange et al., 2008), nicotinamide-adenine-dinucleotide (NAD; Sano et al., 2001; Hara et al., 2002), nicotinic acid–adenine-dinucleotide (NAAD; Tóth and Csanády, 2010), and NAAD-phosphate (NAADP; Beck et al., 2006; Lange et al., 2008; Tóth and Csanády, 2010) were all proposed to activate, whereas AMP was suggested to inhibit (Kolisek et al., 2005) TRPM2 channels. Moreover, strongly synergistic activation of TRPM2 currents by subthreshold concentrations of coapplied ADPR plus cADPR (Kolisek et al., 2005; Beck et al., 2006; Lange et al., 2008), ADPR plus NAADP (Beck et al., 2006; Lange et al., 2008), or ADPR plus H_2O_2 (Kolisek et al., 2005; Lange et al., 2008) outlined TRPM2 as a complex molecular machine at the crossroads of several signaling pathways, uniquely integrating information from the cell's redox status as well as from several nodes of the adenine nucleotide metabolic network. Given the key role of TRPM2 in a range of physiological and pathophysiological processes, it is clearly important to identify the precise subset of nucleotides that act directly on the channel.

The above conclusions were mostly based on whole-cell patch-clamp experiments reporting effects on TRPM2 currents upon intracellular dialysis of putative modulators into intact cells. Because under such conditions the entire cellular machinery for nucleotide metabolism and compartmentalization of both nucleotides and Ca^{2+} are in place, direct effects of a modulator on TRPM2 gating cannot be discerned from indirect effects that modulate TRPM2 activity by changing local ADPR and/or Ca^{2+} concentrations. Moreover, the high (typically millimolar) nucleotide concentrations used in most studies left room for the possibility that minor contaminants in the nucleotide stocks are responsible for some of the observed effects. One biophysical study in which putative modulators were directly applied to the cytosolic face of TRPM2 channels in cell-free inside-out patches found no direct effect on TRPM2 channel gating by H_2O_2, cADPR, and AMP, classifying these three compounds as indirect effectors (Tóth and Csanády, 2010). Of note, adequate interpretation of cADPR effects required prior enzymatic degradation of a substantial ADPR contamination detected in commercially available cADPR batches by treatment with a nucleotide pyrophosphatase (type I; Sigma-Aldrich) specific to linear, as opposed to cyclic, ADPR. Because a similar approach for "purifying" linear pyridine dinucleotide stocks was not available, it still remains an open question as to whether low affinity TRPM2 activation in inside-out patches by directly applied NAAD, NAADP (Tóth and Csanády, 2010), and NAD (Sano et al., 2001; Hara et al., 2002) is truly attributable to the pyridine dinucleotides as opposed to contaminant ADPR. This question is particularly relevant for the most abundant pyridine dinucleotide NAD, cytosolic concentrations of which are in the hundreds-of-micromolar range (Hara et al., 2002).

Here, we take advantage of heterologously expressed purified NUDT9 (Tóth et al., 2014), which specifically degrades ADPR but not pyridine dinucleotides, to enzymatically purify NAD, NAAD, and NAADP from potential contaminants, and exploit the noninactivating T5L TRPM2 variant (Tóth and Csanády, 2012), which allows for long steady-state recordings. Our original aim was to address the true effect of NAD and its dinucleotide analogues on TRPM2 gating by direct cytosolic application of the purified compounds to TRPM2 channels in inside-out patches. In addition, our studies led to the fortuitous discovery of a novel TRPM2 activator.

MATERIALS AND METHODS

Molecular biology

T5L-TRPM2/pGEMHE (Tóth and Csanády, 2012) was linearized with NheI (New England Biolabs, Inc.) and transcribed in vitro using T7 polymerase; cRNA was stored at −80°C.

Isolation and injection of *Xenopus laevis* oocytes

Xenopus oocytes were dissected, separated by collagenase treatment, and stored at 18°C in a Ringer's solution supplemented with 1.8 mM $CaCl_2$ and 50 µg/ml gentamycin. Oocytes were injected with 10 ng cRNA, and recordings were performed 2–3 d after injection.

Excised inside-out patch-clamp recordings

Inward macroscopic TRPM2 channel currents in inside-out patches excised from *Xenopus* oocytes injected with T5L-TRPM2 cRNA were recorded at a temperature of 25°C in symmetrical Na-gluconate–based solutions at a membrane potential of −20 mV, as described previously (Csanády and Törocsik, 2009). Pipette solution contained (mM): 140 Na-gluconate, 2 Mg-gluconate$_2$, and 10 HEPES, pH 7.4 with NaOH (free [Ca^{2+}] of ∼4 µM; the pipette electrode was dipped into a 140-mM NaCl-based solution carefully layered on top). The continuously flowing bath solution (mM: 140 Na-gluconate, 2 Mg-gluconate$_2$, 10 HEPES, pH 7.1 with NaOH, and either 1 mM EGTA [to obtain "zero" (∼8 nM) Ca^{2+}], or 1 mM Ca-gluconate$_2$ [to obtain 125 µM free [Ca^{2+}]]) was controlled by electronic valves and could be exchanged with a time constant of <100 ms. Na-ADPR (Sigma-Aldrich) was added to the

Downloaded from http://rupress.org/jgp/article-pdf/145/5/419/1794700/jgp_201511377.pdf by guest on 07 February 2026

bath from 32 to 200 mM, and ADPR-2′-phosphate (ADPRP; Biolog) or nonpurified dinucleotides (Sigma-Aldrich) from 50 to 200 mM, aqueous stock solutions, followed by adjustment of pH to 7.1 using NaOH. The addition of purified dinucleotides (see below) to the bath solution caused no significant pH changes (<0.1). Currents were amplified and low-pass filtered at 2 kHz, digitized at 10 kHz, and stored to disk (Axopatch 200B, Digidata 1440A, and Pclamp 10; Molecular Devices). For display, currents were digitally filtered at 200 Hz.

Data analysis and statistics

Fractional TRPM2 current activation by various concentrations of nonpurified and purified pyridine dinucleotides or ADPRP was calculated by dividing average steady current in the presence of the test nucleotide to the mean of the steady currents recorded in the same patch during bracketing applications of 32 µM ADPR, all in the presence of saturating (125 µM) cytosolic Ca^{2+}. This procedure yields undistorted dose–response relationships, unaffected by the modest time-dependent decline in T5L-TRPM2 channel activity (see Figs. 1 B, 3, B and C, and 4, B and C), which likely reflects gradual depletion of membrane PIP_2 (Tóth and Csanády, 2012). Dose–response curves were fitted to the Hill equation, and macroscopic current relaxation time courses were fitted to decaying single-exponential functions, by the method of least squares. All data are presented as mean ± SEM from at least 10 measurements.

Purification of the NUDT9 enzyme

Overexpression and purification of human mitochondrial NUDT9 hydrolase was done as described previously (Tóth et al., 2014). In brief, a synthetic gene of mature NUDT9 (residues 59–350), containing a hexahistidine tag at the C terminus and incorporated into the pJ411 plasmid (DNA2.0), was transformed into *Escherichia coli* (BL21 DE3 strain) and induced with 1 mM IPTG for 3 h at 37°C. Cells were harvested and lysed with sonication, and the cleared supernatant was subjected to nickel-affinity purification followed by gel filtration through a Superdex 200 10/300 GL column (GE Healthcare). Protein purity was monitored by SDS PAGE, and the final protein concentration was estimated colorimetrically.

Preparation and enzymatic purification of pyridine dinucleotide solutions

Sodium salts of NAD, NAAD, and NAADP were purchased from Sigma-Aldrich. Stock solutions were prepared at 100–200-mM concentrations in water, and the pH was adjusted with NaOH to values at which the nucleotides possess no significant buffering capacity. To determine such "optimal" target pH values, and the stoichiometries of NaOH necessary to achieve them (in the face of large variations, among different nucleotides, manufacturers, and lot numbers, in sodium content of nucleotide stock powders), we first obtained complete pH titration curves for a 2-mM aqueous solution of each nucleotide batch (Fig. S1). Based on these titration curves, target pH was set to ∼6.5 for NAD (Fig. S1, green curve) and to ∼8.5 for NAAD (Fig. S1, blue curve) and NAADP (Fig. S1, purple curves). For the nucleotide batches used here, the stoichiometry of NaOH necessary to reach the target pH was ∼0 mol/mol for NAD, ∼0.85 mol/mol for NAAD, but ∼2.3 and ∼3.1 mol/mol for two different batches of NAADP (Fig. S1).

To purify each dinucleotide from its ADPR or ADPRP contaminant, 16 mM $MgCl_2$, 50 mM of either MES, pH 6.5 (for NAD), or Tris, pH 8.5 (for NAAD and NAADP), and 1 µM of purified NUDT9 were added to the respective pH-adjusted stock solutions, and the reaction mixtures were incubated for 2 h at room temperature. Successful clearing of contaminating ADPR or ADPRP was monitored by thin-layer chromatography (TLC). For dinucleotide/ADPR competition experiments (Fig. 4), the NUDT9 hydrolase was removed from purified dinucleotide stock solutions by passage through a 5-kD molecular weight cutoff filter (Sartorius), and fractional recovery of dinucleotides was estimated by TLC. Solutions containing mixtures of purified, filtered dinucleotides and 1 µM ADPR (Fig. 4) showed no decline, over several

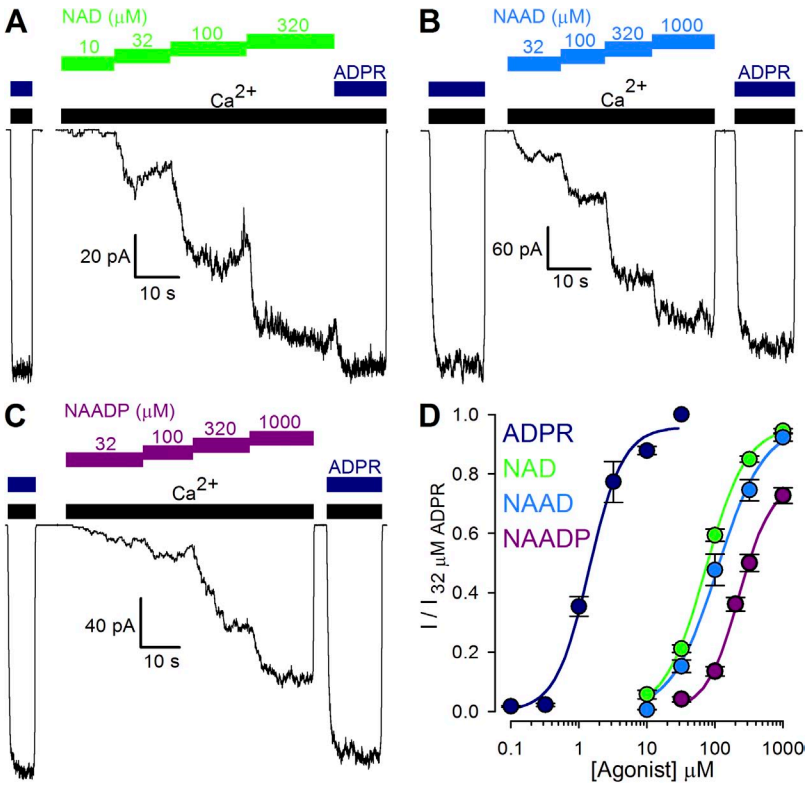

Figure 1. Nonpurified pyridine dinucleotides act as low affinity TRPM2 activators. (A–C) Macroscopic T5L-TRPM2 currents elicited in inside-out patches by cytosolic application of saturating (125 µM) Ca^{2+} (black bars) and either 32 µM ADPR (dark blue bars) or increasing concentrations of nonpurified NAD (A, green bars), NAAD (B, blue bars), or NAADP (C, purple bars). (D) Dose–response curves for fractional current activation by ADPR (dark blue; replotted from Tóth and Csanády, 2012), and nonpurified NAD (green), NAAD (blue), and NAADP (purple). Currents were normalized to those measured in 32 µM ADPR. Solid lines are fits to the Hill equation yielding $K_{1/2}$ = 1.4 ± 0.1 µM, n = 1.8 ± 0.2, and $I_{rel;\infty}$ = 0.96 ± 0.03 for ADPR; $K_{1/2}$ = 73 ± 3 µM, n = 1.4 ± 0.1, and $I_{rel;\infty}$ = 0.96 ± 0.01 for NAD; $K_{1/2}$ = 109 ± 17 µM, n = 1.3 ± 0.2, and $I_{rel;\infty}$ = 0.96 ± 0.06 for NAAD; and $K_{1/2}$ = 226 ± 19 µM, n = 1.8 ± 0.2, and $I_{rel;\infty}$ = 0.78 ± 0.04 for NAADP. Error bars represent mean ± SEM.

Downloaded from http://rupress.org/jgp/article-pdf/145/5/419/1794700/jgp_201511377.pdf by guest on 07 February 2026

hours, in their efficiency to cause fractional TRPM2 current activation, confirming complete removal of the hydrolase by the filtering process (compare Tóth and Csanády, 2010). Purified and purified/filtered dinucleotide stocks were stored at −80°C.

TLC

The compositions of nucleotide preparations were verified on either Polygram SIL G/UV_{254} (Macherey-Nagel) or Silica gel 60 F_{254} (Merck) TLC plates. Aliquots (1 µl) from each nucleotide sample were spotted on the TLC sheet and dried. TLC plates were developed in 22 different developing solutions, in an attempt to best resolve specific components of each particular sample. Developing solutions used in the figures shown (indicated in the figure legends) were DS1 (0.2 M ammonium bicarbonate in water/ethanol = 3:7 [vol/vol]), DS2 (3.3 M ammonium formate, 4.2% boric acid, pH 7.0 with NH_4OH), and DS3 (1 M LiCl, 6% boric acid, pH 7.0 with NH_4OH). Nucleotides were visualized under UV light.

TLC image processing

All TLC images are presented in grayscale after modification on luminosity and contrast for the sole purpose of better visualization of weaker spots in the samples. Such adjustments are homogenous across each image, and illumination/contrast gradients were not used. Some TLC images were vertically split, and the lanes are presented in rearranged order for the sake of symmetry in sample order.

Mass spectrometry

Electrospray ionization time-of-flight mass spectrometry analysis of purified dinucleotide samples was done at the mass spectrometry core facility of the Department of Organic Chemistry, Eötvös Loránd University (Budapest, Hungary).

Online supplemental material

Fig. S1 shows pH titration curves of all studied nucleotides, demonstrating the different pH-buffering capacity and variable sodium content of commercial preparations. Fig. S2 demonstrates time-dependent formation of ADPR from NAD by spontaneous hydrolysis in buffered aqueous solutions. Fig. S3 compares chromatographic mobilities of nonpurified and purified dinucleotides on nonoverloaded TLC sheets. The online supplemental material is available at http://www.jgp.org/cgi/content/full/jgp.201511377/DC1.

RESULTS

Nonpurified pyridine dinucleotides act as low affinity TRPM2 activators

To directly compare the potencies and efficacies of various pyridine dinucleotides toward stimulation of TRPM2 gating, we examined fractional activation of inward macroscopic TRPM2 currents by increasing concentrations of NAD (Fig. 1 A, green bars), NAAD (Fig. 1 B, blue bars), and NAADP (Fig. 1 C, purple bars), supplied directly to the cytosolic faces of inside-out patches excised from *Xenopus* oocytes expressing human T5L-TRPM2. All nucleotides were applied in the continued presence of saturating (125 µM; compare Tóth and Csanády, 2012) cytosolic Ca^{2+} (Fig. 1, A–C, black bars), and activated steady currents were normalized to those elicited in the same patch by bracketing exposures to saturating (32 µM; compare Tóth and Csanády, 2012) ADPR (Fig. 1, A–C, dark blue bars). Consistent with previous reports (Sano et al., 2001; Hara et al., 2002; Tóth and Csanády, 2010), all three pyridine dinucleotides readily opened TRPM2 channels, but with apparent affinities about two orders of magnitude lower than for ADPR (Fig. 1 D; fitted $K_{1/2}$ values were 1.4 ± 0.1 µM for ADPR [dark blue symbols], 73 ± 3 µM for NAD [green symbols], 109 ± 17 µM for NAAD [blue symbols], and 226 ± 19 µM for NAADP [purple symbols]). Moreover, whereas TRPM2 channels were fully activated by saturating concentrations of NAD and NAAD, currents in saturating NAADP approached only 78 ± 4% of those in 32 µM ADPR (Fig. 1 D, purple fit line).

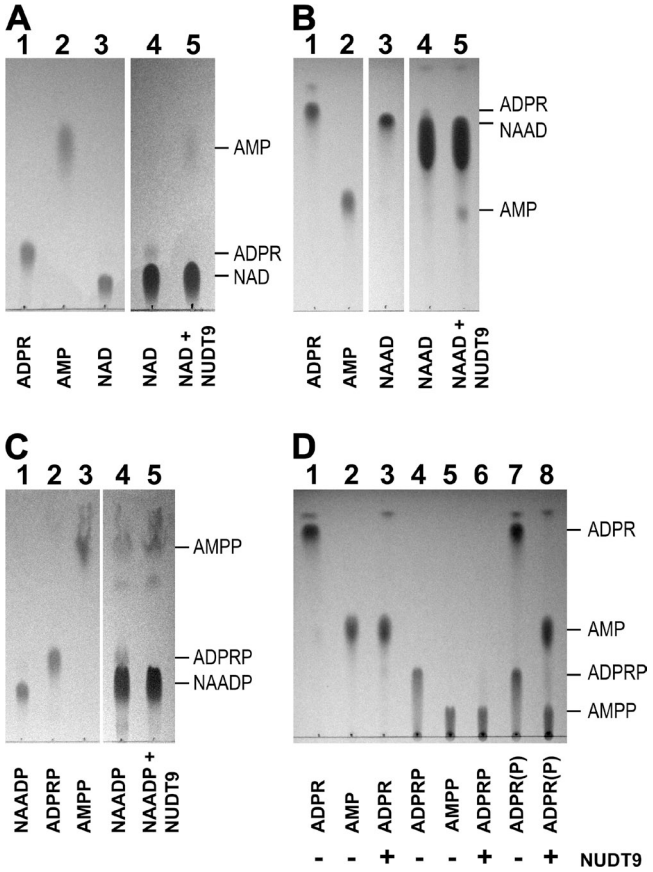

Figure 2. Enzymatic treatment efficiently removes ADPR and ADPRP contamination of pyridine dinucleotides. (A–C) TLC images showing the purification of (A) NAD, (B) NAAD, and (C) NAADP. Loaded samples (1 µl) were as follows: (A) 10 mM ADPR (lane 1), 10 mM AMP (lane 2), 10 mM NAD (lane 3), and 100 mM NAD before (lane 4) and after (lane 5) treatment with NUDT9. (B) 10 mM ADPR (lane 1), 10 mM AMP (lane 2), 10 mM NAAD (lane 3), and 100 mM NAAD before (lane 4) and after (lane 5) treatment with NUDT9. (C) 10 mM NAADP (lane 1), 10 mM ADPRP (lane 2), 10 mM AMPP (lane 3), and 100 mM NAADP before (lane 4) and after (lane 5) treatment with NUDT9. (D) Hydrolytic activity of NUDT9 on ADPR and ADPRP, showing 10 mM ADPR (lane 1), 10 mM AMP (lane 2), 10 mM ADPR treated with NUDT9 (lane 3), 10 mM ADPRP (lane 4), 10 mM AMPP (lane 5), 10 mM ADPRP treated with NUDT9 (lane 6), mixture of 10 mM ADPR and 10 mM ADPRP before (lane 7), and after (lane 8) treatment with NUDT9. Developing solution was DS2 in A and C, and DS1 in B and D.

Downloaded from http://rupress.org/jgp/article-pdf/145/5/419/1794700/jgp_201511377.pdf by guest on 07 February 2026

Enzymatic treatment efficiently removes ADPR and ADPRP contamination of pyridine dinucleotides detectable by TLC

Commercial preparations of NAD were reported to contain significant amounts of contaminant ADPR (Tóth and Csanády, 2010). To efficiently monitor selective removal of this contamination by treatment with the purified NUDT9 hydrolase, which cleaves ADPR into AMP and ribose-5-phosphate (Tóth et al., 2014; Fig. 2 D, lanes 1–3; ribose-5-phosphate is not fluorescent and therefore invisible), we used a TLC developing solution (DS2; see Materials and methods), which causes clear separation of all three spots corresponding to NAD, ADPR, and AMP (loaded as 1-µl aliquots of 10-mM solutions; Fig. 2 A, lanes 1–3). Loading a 10-fold excess of NAD (Fig. 2 A, lane 4) indeed allowed clear detection of a faint spot co-migrating with ADPR; NUDT9 treatment eliminated this impurity and caused the appearance of a novel spot corresponding to AMP (Fig. 2 A, lane 5), confirming stoichiometric cleavage of ADPR by the enzyme.

A similarly optimal developing solution was not found for NAAD: although DS1 (see Materials and methods) causes good separation of NAAD and AMP, even partial separation of NAAD from barely faster ADPR requires very long runs (Fig. 2 B, lanes 1–3). This might explain why ADPR contamination of NAAD was not detected in our earlier study using DS1 (Tóth and Csanády, 2010). However, when NAAD is loaded at a 10-fold excess, upon prolonged development a previously overlooked faint halo becomes discernible at the leading edge of the NAAD spot (Fig. 2 B, lane 4). Moreover, that diffuse shadow disappears upon NUDT9 treatment, synchronously with the appearance of a novel spot co-migrating with AMP (Fig. 2 B, lane 5). These findings confirm that commercial NAAD also contains substantial contamination by ADPR, which can be removed by NUDT9 treatment.

Because NAADP and ADPR are well separated in DS1 developing solution, the lack of an ADPR spot even when loading large quantities of NAADP (Tóth and Csanády, 2010) suggests that this nucleotide is indeed devoid of an ADPR impurity—at least at the level of detection by TLC. One potential source of impurities in pyridine dinucleotide stocks might be spontaneous cleavage of the pyridine base from the distal ribose. Indeed, at least in solution and at room temperature, we could confirm spontaneous degradation of NAD into ADPR over the time course of days (Fig. S2 A), a process accelerated at slightly basic pH (Fig. S2 B). If that process was indeed the main source of ADPR in our NAD and NAAD stocks, this would explain the lack of such impurity in NAADP. Because the latter contains an additional phosphate at the 2′ position of the proximal ribose, loss of the pyridine base would generate ADPRP instead of ADPR. Interestingly, we found that the NUDT9 hydrolase also cleaves ADPRP (into AMP-2′-phosphate [AMPP] and ribose-5-phosphate), whether

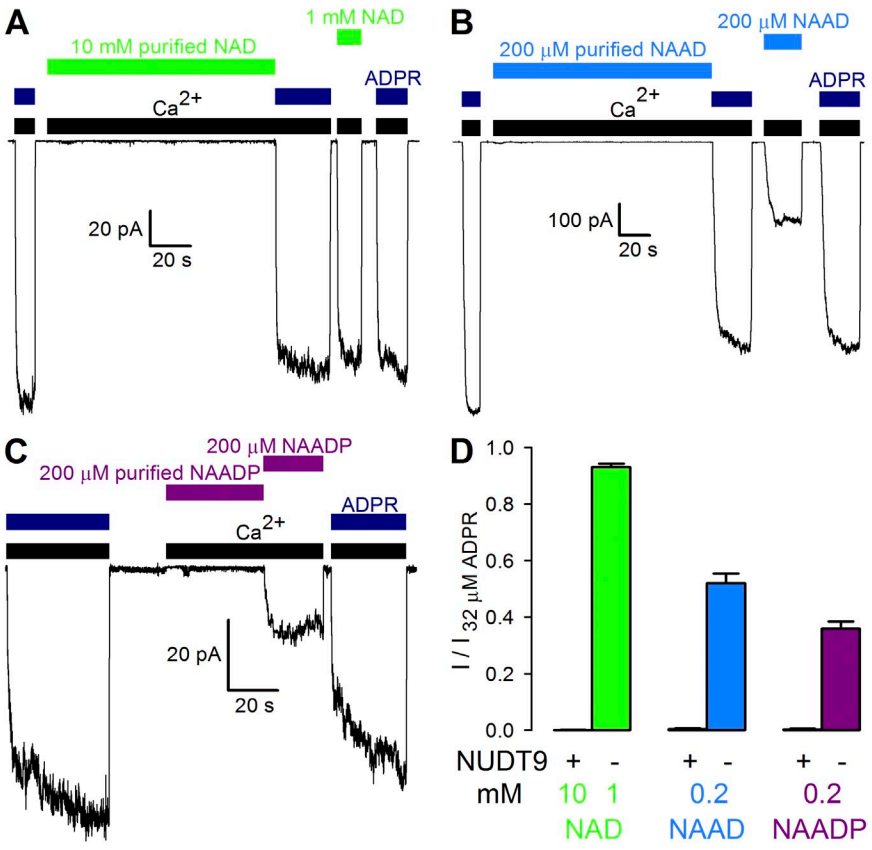

Figure 3. Purified pyridine dinucleotides do not activate TRPM2 channels even at very high concentrations. (A–C) Macroscopic T5L-TRPM2 currents evoked by cytosolic application of saturating Ca^{2+} (black bars) and either 32 µM ADPR (dark blue bars) or high concentrations of untreated or NUDT9-treated ("purified") NAD (A, green bars), NAAD (B, blue bars), or NAADP (C, purple bars). (D) Fractional current activation by indicated concentrations (mM) of NUDT9-treated ("+") or nonpurified ("−") NAD (green), NAAD (blue), and NAADP (purple). Currents were normalized to those measured in 32 µM ADPR. Error bars represent mean ± SEM.

Downloaded from http://rupress.org/jgp/article-pdf/145/5/419/1794700/jgp_201511377.pdf by guest on 07 February 2026

tested in isolation (Fig. 2 D, lanes 4–6) or as a mixture with ADPR (Fig. 2 D, lanes 7 and 8). Thus, we reasoned that NUDT9 could also be used for the removal of any potential ADPRP impurity from NAADP. Indeed, using DS2 developing solution, which provides clear separation of NAADP, ADPRP, and AMPP spots (Fig. 2 C, lanes 1–3), loading a 10-fold excess of NAADP reveals distinct shadows co-migrating with both ADPRP and AMPP (Fig. 2 C, lane 4); the former spot is eliminated by NUDT9 treatment, whereas the density of the latter spot synchronously increases (Fig. 2 C, lane 5). Thus, although NAADP stocks are devoid of ADPR, they instead contain ADPRP, which is also removable by NUDT9 treatment.

Importantly, as expected, NUDT9 treatment did not alter the mobilities of the three pyridine dinucleotides (Fig. 2, A–C, lanes 4 and 5; also see Fig. S3 for TLC images of purified vs. nonpurified dinucleotides without overloading), suggesting that NAD, NAAD, and NAADP remained intact during the purification procedure, a conclusion further confirmed by electrospray ionization time-of-flight mass spectrometry analysis of the purified samples.

Purified pyridine dinucleotides fail to activate TRPM2 channels even at very high concentrations

Our enzymatically purified pyridine dinucleotide solutions allowed us to address for the first time whether the dinucleotides themselves possess any potential for supporting TRPM2 channel gating. Interestingly, superfusion with a bath solution containing saturating Ca^{2+} (Fig. 3, A–C, black bars) and high concentrations of purified NAD (Fig. 3 A), NAAD (Fig. 3 B), or NAADP (Fig. 3 C) consistently failed to cause TRPM2 channel openings in inside-out patches, even though subsequent application of the respective nonpurified dinucleotide, or of 32 µM ADPR (Fig. 3, A–C, dark blue bars), elicited macroscopic TRPM2 currents in each case. Whereas fractional activation by each nonpurified dinucleotide (Fig. 3 D, bars labeled "−") conformed to that expected from the respective dose–response curve (Fig. 1 D), average currents in the presence of each purified dinucleotide remained identically zero (Fig. 3 D, bars labeled "+"). Thus, NAD, NAAD, and NAADP are no direct TRPM2 activators.

Purified pyridine dinucleotides do not affect activation of TRPM2 channels by subsaturating ADPR

Failure of the pyridine dinucleotides to activate TRPM2 reflects their inability either to bind to the channel or to stabilize the open-pore conformation. In the latter case, however, their presence should inhibit TRPM2 activation by ADPR, by competition for a common binding site. To address this possibility, fractional current activation by a subsaturating concentration of 1 µM ADPR alone was compared with that elicited by a mixture of 1 µM ADPR and high concentrations of purified NAD (Fig. 4 A), NAAD (Fig. 4 B), or NAADP (Fig. 4 C).

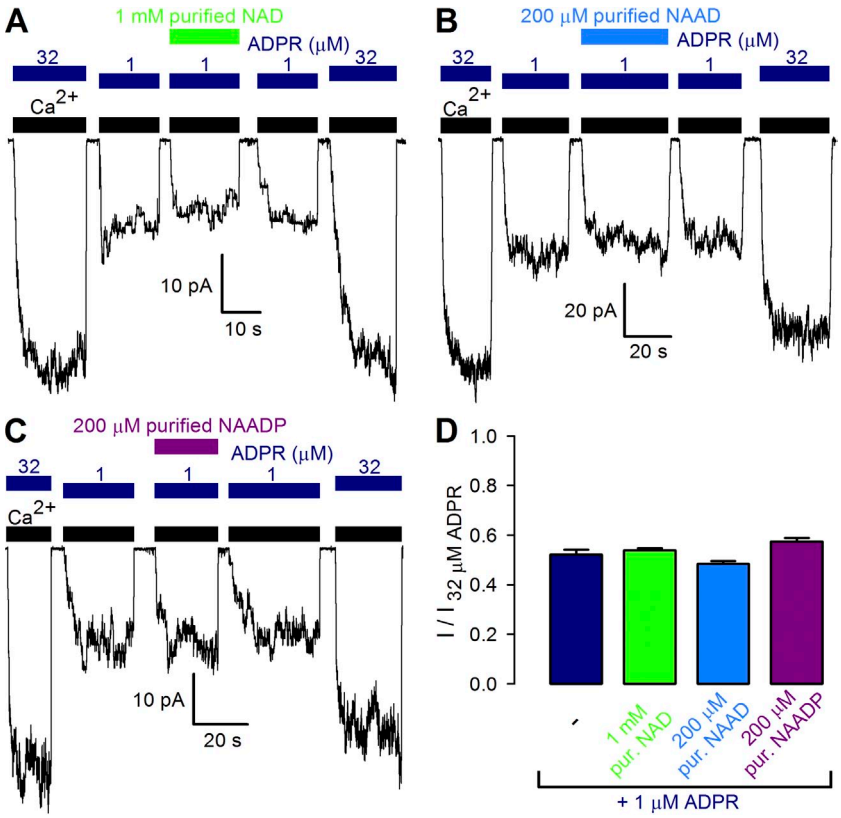

Figure 4. Purified pyridine dinucleotides do not compete activation of TRPM2 channels by ADPR. (A–C) Macroscopic T5L-TRPM2 currents elicited by cytosolic application of saturating Ca^{2+} (black bars) and either 32 or 1 µM ADPR (dark blue bars) alone, or a mixture of 1 µM ADPR with a high concentration of NUDT9-treated, filtered ("purified") NAD (A, green bar), NAAD (B, blue bar), or NAADP (C, purple bar). (D) Fractional current activation by 1 µM ADPR alone (dark blue) or in combination with indicated concentrations of NUDT9-treated, filtered NAD (green), NAAD (blue), and NAADP (purple). Currents were normalized to those measured in 32 µM ADPR. Error bars represent mean ± SEM.

Downloaded from http://rupress.org/jgp/article-pdf/145/5/419/1794700/jgp_201511377.pdf by guest on 07 February 2026

However, fractional currents in 1 µM ADPR (Fig. 4 D, dark blue bar) remained unaffected by the presence of either dinucleotide (Fig. 4 D, green, blue, and purple bars). These results suggest that NAD, NAAD, and NAADP fail to activate TRPM2 because they do not fit into the ADPR-binding cleft on NUDT9H. They also refute a direct mechanism for the reported strong positive cooperativity between ADPR and NAADP for TRPM2 activation in intact cells (Beck et al., 2006; Lange et al., 2008).

ADPRP is a novel true TRPM2 partial agonist with distinctive kinetic features

In light of the lack of TRPM2 stimulation by NUDT9-treated NAADP (Fig. 3 C) and the lack of ADPR contamination in the untreated NAADP stock (Tóth and Csanády, 2010), contaminating ADPRP (Fig. 2 C, lane 4) seemed the most likely candidate responsible for TRPM2 stimulation by nonpurified NAADP (Fig. 1 C). Indeed, in inside-out patches, in the presence of saturating Ca^{2+} (Fig. 5 A, black bars), the application of increasing concentrations of ADPRP (Fig. 5 A, red bars) activated macroscopic TRPM2 currents in a dose-dependent manner. The dose–response curve for fractional current activation by ADPRP (Fig. 5 B, red symbols and fit line) yielded a $K_{1/2}$ of 13 ± 1 µM, reporting an ∼10-fold lower apparent affinity compared with ADPR (Fig. 5 B, dark blue symbols and fit line). Of note, even in saturating ADPRP, TRPM2 currents remained distinctly smaller than in 32 µM ADPR (Fig. 5 A). Because unitary current amplitudes of channels activated by ADPR or ADPRP were indistinguishable (−1.45 ± 0.02 pA [n = 5] and −1.45 ± 0.02 pA [n = 5], respectively, at a membrane potential of −20 mV), the reduced macroscopic current in ADPRP necessarily reflects a reduction in open probability, suggesting that the maximal efficacy of ADPRP for stimulating channel open probability is only 83 ± 2% (Fig. 5 B, red fit line) of that of ADPR.

To dissect the kinetic reason for the smaller open probability of TRPM2 channels when gated by ADPRP, we compared macroscopic current decay rates upon sudden removal of activating ADPRP or ADPR in the maintained presence of saturating Ca^{2+} (Fig. 5 C): the time constant (τ) of the decaying current is a convenient measure of the average lifetime of a channel open burst, elicited by binding of the respective nucleotide (Tóth et al., 2014). Time constants of single exponentials fitted to the current decay time courses after ADPRP removal (Fig. 5 C, red curves, with τ given in seconds) were consistently smaller than those obtained upon ADPR removal (Fig. 5 C, dark blue curves); on average, the estimated mean burst duration of TRPM2 channels was approximately threefold shorter when they were opened by ADPRP as opposed to ADPR (Fig. 5 D, compare red and blue bars).

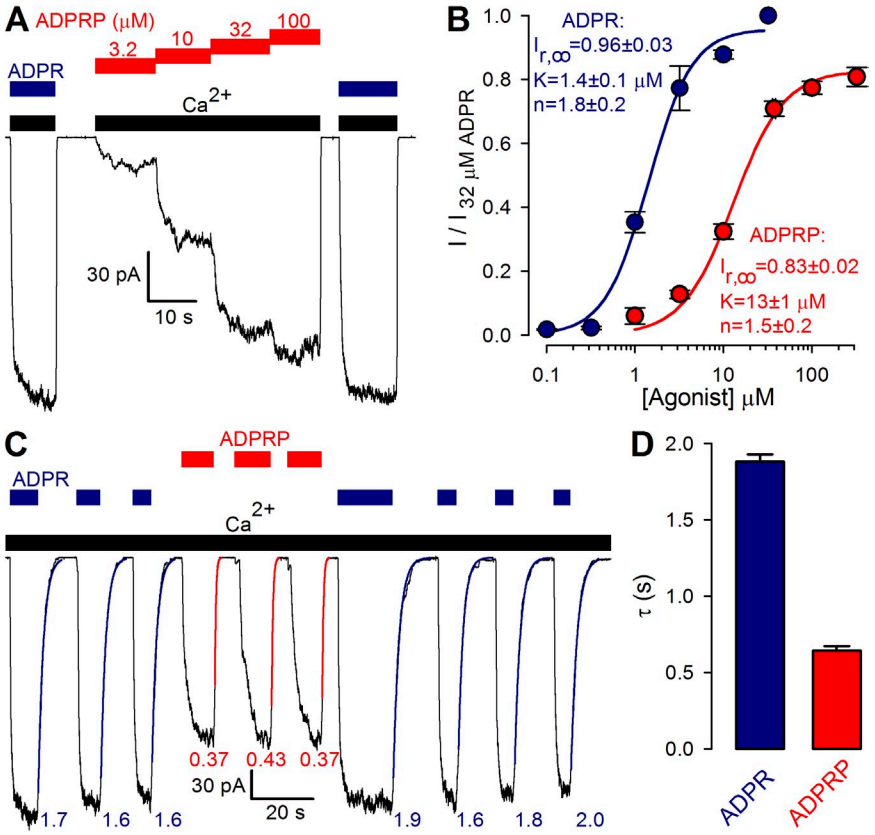

Figure 5. ADPRP is a novel true TRPM2 partial agonist with distinctive kinetic features. (A) Macroscopic T5L-TRPM2 currents in response to cytosolic application of saturating Ca^{2+} (black bars) and either 32 µM ADPR (dark blue bars) or increasing concentrations of ADPRP (red bars). (B) Dose–response curves for fractional current activation by ADPR (dark blue; replotted from Fig. 1 D) and ADPRP (red). Currents were normalized to those measured in 32 µM ADPR. Solid lines are fits to the Hill equation with parameters plotted in the panel. (C) Macroscopic T5L-TRPM2 current repeatedly activated by brief exposures to 32 µM ADPR (dark blue bars) or 100 µM ADPRP (red bars), in the continued presence of saturating Ca^{2+} (black bars). Current decay time courses upon nucleotide removal were fitted by single-exponential functions (colored curves) with time constants indicated (in seconds). (D) Average T5L-TRPM2 current relaxation time constants (in seconds) upon sudden removal of saturating ADPR (dark blue) or ADPRP (red) in the maintained presence of Ca^{2+}. Error bars represent mean ± SEM.

Downloaded from http://rupress.org/jgp/article-pdf/145/5/419/1794700/jgp_201511377.pdf by guest on 07 February 2026

Kinetic fingerprint betrays active contaminant of nonpurified pyridine dinucleotides

If TRPM2 activation by nonpurified pyridine dinucleotides was indeed caused by their ADPR or ADPRP contaminations, then the kinetics of gating in each untreated dinucleotide should reflect the properties of the respective contaminant. In particular, macroscopic closing rates upon sudden removal of nonpurified dinucleotides should betray which of the two contaminants is responsible for channel gating. Indeed, in experiments in which macroscopic TRPM2 currents were repeatedly activated by brief exposures to saturating concentrations of ADPR or various nonpurified pyridine dinucleotides, single-exponential fits to current decay time courses upon removal of nonpurified NAD (Fig. 6 A, green curves) or NAAD (Fig. 6 B, blue curves) yielded time constants (Fig. 6, A and B, green and blue numbers) identical to those upon removal of ADPR (Fig. 6, A and B, dark blue fit lines and numbers; compare Fig. 6 D, left group of bars). In contrast, removal of nonpurified NAADP resulted in approximately threefold faster current decay (Fig. 6 C, purple vs. dark blue curves), with a time constant identical to that obtained for channel deactivation after removal of ADPRP (Fig. 6 D, purple vs. red bars).

DISCUSSION

Soon after the discovery of ADPR as the primary activator of TRPM2 (Perraud et al., 2001; Sano et al., 2001), a multitude of further adenine nucleotides were screened for potential modulatory effects on the channel. These studies reported effects on TRPM2 whole-cell currents by intracellular dialysis of intact cells with the test compounds. In particular, whereas NADH and NADP were found ineffective (Hara et al., 2002), cADPR (Beck et al., 2006; Lange et al., 2008), NAD (Sano et al., 2001; Hara et al., 2002), NAAD (Tóth and Csanády, 2010), and NAADP (Beck et al., 2006; Lange et al., 2008; Tóth and Csanády, 2010) were all found to activate TRPM2, and AMP was proposed to act as an inhibitor (Kolisek et al., 2005). Furthermore, strongly synergistic effects between ADPR and cADPR (Kolisek et al., 2005; Beck et al., 2006; Lange et al., 2008) or ADPR and NAADP (Beck et al., 2006; Lange et al., 2008) delineated intricate mechanisms for fine-tuning TRPM2 activity in cells. This intriguing position of TRPM2 at the crossroads of the complex network of adenine nucleotide metabolism (Malavasi et al., 2008; Koch-Nolte et al., 2009) and the multiple roles of TRPM2 in apoptosis (Hara et al., 2002; Kaneko et al., 2006; Olah et al., 2009), immunocyte activation (Yamamoto et al., 2008), and insulin secretion (Uchida et al., 2011) underscore the importance of identifying the precise subset of nucleotides that act directly on the TRPM2 protein and their exact effects on channel gating.

From the multitude of proposed nucleotide modulators, previous work using direct application to inside-out patches of AMP and enzymatically purified cADPR

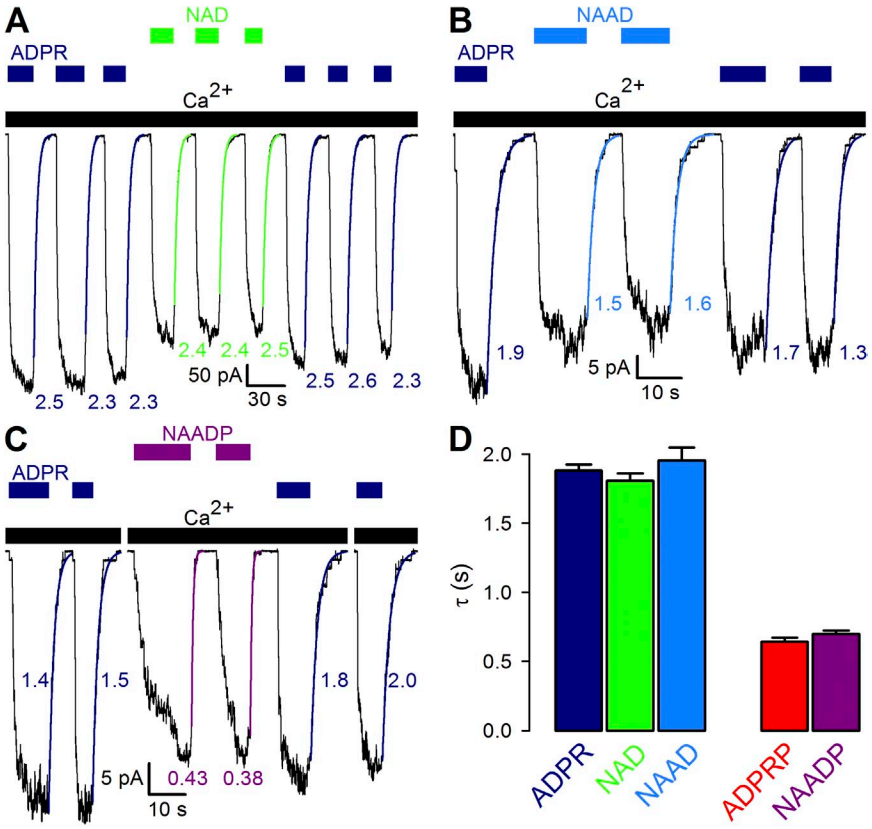

Figure 6. Kinetic fingerprint betrays active contaminant of nonpurified pyridine dinucleotides. (A–C) Macroscopic T5L-TRPM2 current repeatedly activated by brief exposures to 32 µM ADPR (dark blue bars) or saturating concentrations of nonpurified NAD (1 mM; A, green bars), NAAD (1 mM; B, blue bars), or NAADP (2 mM; C, purple bars) in the continued presence of saturating Ca^{2+} (black bars). Current decay time courses upon nucleotide removal were fitted by single-exponential functions (colored curves), with time constants indicated (in seconds). (D) Average T5L-TRPM2 current relaxation time constants (in seconds) upon sudden removal of saturating NAD (green), NAAD (blue), or NAADP (purple) in the maintained presence of Ca^{2+}. Analogous parameters for ADPR (dark blue) and ADPRP (red) are replotted from Fig. 5 D for comparison. Error bars represent mean ± SEM.

Downloaded from http://rupress.org/jgp/article-pdf/145/5/419/1794700/jgp_201511377.pdf by guest on 07 February 2026

firmly ruled out these two nucleotides as direct TRPM2 effectors (Tóth and Csanády, 2010). In particular, activation by commercial cADPR was clearly attributable to contaminant ADPR, which could be removed by a commercially available nucleotide pyrophosphatase specific to linear, as opposed to cyclic, ADPR analogues. Because efficient tools for purifying linear pyridine dinucleotides were unavailable and ADPR contamination of NAAD and NAADP stocks could not be detected, those two pyridine dinucleotides were concluded to be low affinity direct TRPM2 activators. Recently, we have expressed and affinity purified NUDT9, a highly specific mitochondrial ADPRase (Tóth et al., 2014). Availability of this enzyme, combined with cell-free inside-out patch-clamp technology using rapid direct application of test compounds to the cytosolic membrane surface, allowed us to address for the first time whether pure pyridine dinucleotides can indeed directly interact with, and regulate gating of, TRPM2 channels.

Using enhanced TLC technology, we demonstrate here that commercially available pyridine dinucleotide preparations contain significant contamination by the respective nucleotide analogue lacking the pyridine base (~2, 1, and 5%, respectively, in the NAD, NAAD, and NAADP batches studied here). Whereas in living cells these products, ADPR and ADPRP, are generated by the enzyme CD38 (Aarhus et al., 1995; Schmid et al., 2011; Fig. 7, left), one probable source of such contamination in commercial preparations is spontaneous cleavage of the pyridine base (Fig. S2). We also establish here that NUDT9, known as a specific ADPRase (Lin et al., 2002), degrades ADPRP as completely as it does ADPR (Fig. 7, right; compare Fig. 2 D).

We show here for the first time that pyridine dinucleotides themselves are incapable of activating TRPM2 channels (Fig. 3), even at concentrations orders of magnitude higher than their typical cytosolic values, which are submillimolar for NAD (Hara et al., 2002), and low nanomolar for NAADP (Churamani et al., 2004; Fliegert et al., 2007). In principle, this lack of effect of pyridine dinucleotides on TRPM2 might reflect their inability either to bind to the NUDT9H domain or to promote the conformational change associated with pore opening. In the latter case, however, NAD analogues should act as inverse agonists, competing channel activation by ADPR. Because no such effects could be demonstrated for any of the three pyridine dinucleotides tested (Fig. 4), we conclude that NAD, NAAD, and NAADP do not activate TRPM2 because they do not bind to the NUDT9H domain. Furthermore, because none of the dinucleotides caused sensitization toward ADPR activation in our cell-free patches (Fig. 4), reported synergistic effects between NAADP and ADPR in intact cells (Beck et al., 2006; Lange et al., 2008) must

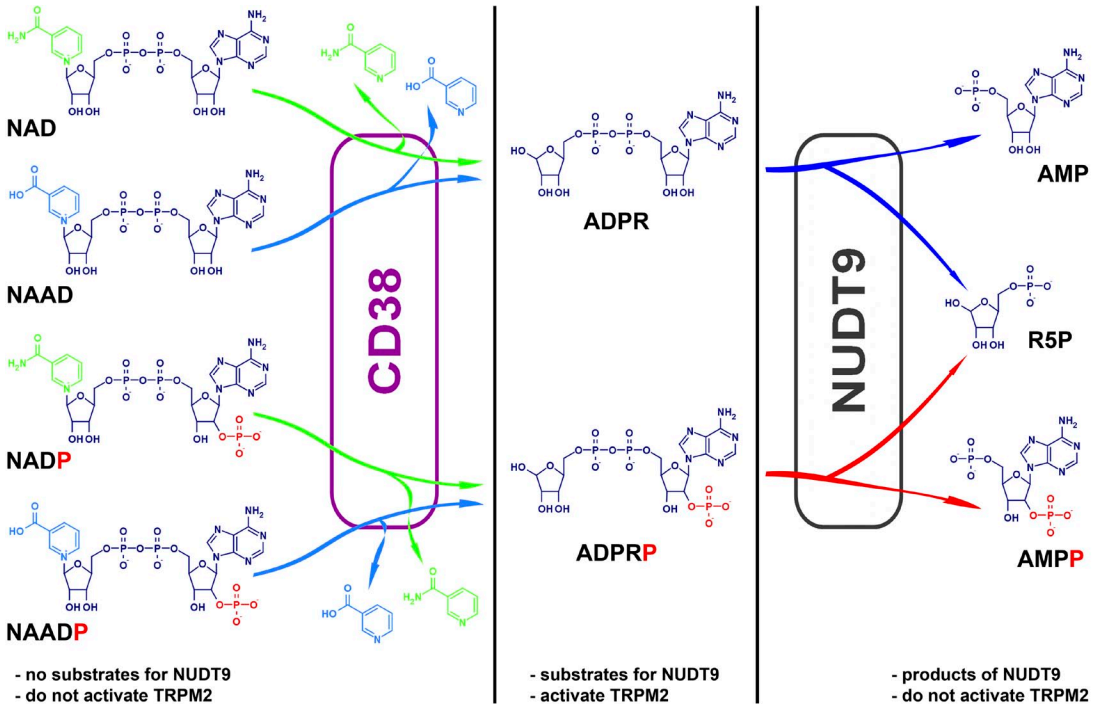

Figure 7. Summary of nucleotide structures and metabolic pathways of interconversion. Color coding: dark blue, ADPR core structure; green, nicotinamide; blue, nicotinic acid; red, 2′-phosphate. In living cells, ADPR and ADPRP are generated from pyridine dinucleotide precursors by the multifunctional enzyme CD38, and degraded into AMP(P) and ribose-5-phosphate by NUDT9. NUDT9 substrates are also activators of TRPM2.

Downloaded from http://rupress.org/jgp/article-pdf/145/5/419/1794700/jgp_201511377.pdf by guest on 07 February 2026

reflect some indirect effect of NAADP on the local concentrations of true TRPM2 agonists. For instance, NAADP is a long-known potent Ca^{2+}-mobilizing agent, which releases Ca^{2+} from acidic organelles (Fliegert et al., 2007), although its exact molecular target is still controversial (Brailoiu et al., 2009; Calcraft et al., 2009, but compare Wang et al., 2012). Thus, NAADP might modulate TRPM2 activity in cells by elevating local cytosolic $[Ca^{2+}]$.

Consistent with spontaneous cleavage of the pyridine base as the source of the active contaminant in dinucleotide stocks, our TLC analysis detected ADPRP—but no ADPR—contamination in NAADP. Loss of TRPM2 activation by NAADP upon its enzymatic purification (Fig. 3, C and D) strongly suggested that ADPRP might itself act as a TRPM2 agonist. Indeed, direct exposure of channels to ADPRP effectively stimulated gating (Fig. 5 A). Although one might imagine that this stimulation is again caused by some minor ADPR contamination of this nucleotide, two facts argue against such an interpretation and suggest that ADPRP is itself a direct TRPM2 activator. First, to account for the apparent affinity of ADPRP for TRPM2 activation ($K_{1/2}$ of ∼13 µM; Fig. 5 B), only 10-fold lower than that of ADPR ($K_{1/2}$ of ∼1.4 µM; Fig. 1 D), ∼10% contaminant ADPR in our ADPRP stock would have to be postulated. Such a strong contamination would have been clearly detectable by TLC but was not observed (e.g., Fig. 2 D). Second, the kinetics of channel gating in ADPRP was clearly distinct from that in ADPR: compared with the latter, ADPRP supported a smaller channel open probability even when applied at saturating concentrations, as revealed by maximum currents only ∼80% of those elicited by 32 µM ADPR (Fig. 5, A and B). This partial agonist effect of ADPRP, as compared with ADPR, was associated with approximately threefold faster closing rate upon nucleotide removal (Fig. 5, C and D), just as reported for the nonhydrolyzable ADPR analogue AMPCPR in which the oxygen bridging the two phosphates is replaced by a methylene group (Tóth et al., 2014). The relatively modest depression of open probability (P_o) by a threefold acceleration of closing rate is quantitatively explained by the very high P_o of TRPM2 in saturating ADPR: for T5L-TRPM2 channels gating in 32 µM ADPR, steady-state single-channel mean open burst (τ_b) and closed interburst (τ_{ib}) durations are ∼5 and ∼1 s, respectively, and P_o is ∼0.83 ($P_o \sim \tau_b/(\tau_b+\tau_{ib})$) (Tóth et al., 2014). Of note, for both ADPR and AMPCPR, mean burst durations were found to be sensitive to nucleotide concentration, with steady-state τ_b in saturating nucleotide being substantially longer than the macroscopic decay time constant after nucleotide removal (the latter reports τ_b in the absence of nucleotide; Tóth et al., 2014). Assuming that, for ADPRP, steady-state τ_b in saturating nucleotide is similarly shortened as the time constant upon its removal (approximately threefold; Fig. 5 D), we estimate a τ_b of ∼1.8 s in saturating ADPRP. This shortened τ_b, without any change in τ_{ib}, predicts a maximal P_o of ∼0.64 in ADPRP, which is ∼77% of that measured in saturating ADPR and so fully accounts for our observations (Fig. 5 B). Thus, just like AMPCPR, ADPRP is a partial agonist because it is less efficient than ADPR in stabilizing the open (bursting) state. This distinctive kinetic fingerprint of ADPRP is also clearly identifiable in channels gated by nonpurified NAADP (Fig. 6, C and D).

Our enzymatically purified NAD and NAAD solutions also contain the NUDT9 breakdown products AMP and ribose-5-P (Fig. 7), and purified NAADP contains AMPP. Moreover, if the source of contaminating ADPR(P) is indeed spontaneous cleavage of the pyridine base (see Fig. S2), then these bases, nicotinamide and nicotinic acid (Fig. 7, green and blue), must also be present in both our unpurified and purified dinucleotide preparations. Finally, TLC analysis of various nucleotides in a range of different developing solutions revealed other, unidentified spots (e.g., in ADPR: Fig. 2 D, lane 1, top; in NAADP: Fig. 2 C, lane 4, middle), which resisted NUDT9 treatment. However, because all NUDT9-treated nucleotides proved inert toward TRPM2, it can be safely concluded that neither of ribose-5-P, AMP, AMPP, nicotinamide, nicotinic acid, nor any of the unidentified impurities directly affect TRPM2 channels (compare Tóth and Csanády, 2010).

Besides their physiological implications, our findings deepen current understanding of structure–activity relationships in TRPM2 activators (Moreau et al., 2013). Specifically, we conclude that a pyridine substitution at position 1′ of the distal ribose in ADPR (Fig. 7, green and blue) is incompatible with NUDT9H binding, whereas the presence of a phosphate group at the 2′ position of the proximal ribose (Fig. 7, red) is tolerated. Furthermore, NUDT9H and NUDT9 appear to possess similar substrate specificities: NUDT9 substrates are also TRPM2 activators, whereas compounds that do not affect TRPM2 gating are also not substrates for NUDT9.

In conclusion, we have shown here that the pyridine dinucleotides NAD, NAAD, and NAADP do not directly affect TRPM2 activity, because they are unable to bind to the NUDT9H domain. In addition, we have identified ADPRP as a novel TRPM2 agonist. Further studies will have to unravel the in vivo role of ADPRP, as well as the relative contributions of ADPR and ADPRP to the regulation of TRPM2 activity under various physiological and pathophysiological conditions.

This work is supported by an International Early Career Scientist grant from the Howard Hughes Medical Institute to L. Csanády, and MTA Lendület grant LP2012-39/2012.

The authors declare no competing financial interests.

Sharona E. Gordon served as editor.

Submitted: 2 February 2015
Accepted: 17 March 2015

Downloaded from http://rupress.org/jgp/article-pdf/145/5/419/1794700/jgp_201511377.pdf by guest on 07 February 2026

REFERENCES

Aarhus, R., R.M. Graeff, D.M. Dickey, T.F. Walseth, and H.C. Lee. 1995. ADP-ribosyl cyclase and CD38 catalyze the synthesis of a calcium-mobilizing metabolite from NADP. *J. Biol. Chem.* 270:30327–30333. http://dx.doi.org/10.1074/jbc.270.51.30327

Beck, A., M. Kolisek, L.A. Bagley, A. Fleig, and R. Penner. 2006. Nicotinic acid adenine dinucleotide phosphate and cyclic ADP-ribose regulate TRPM2 channels in T lymphocytes. *FASEB J.* 20:962–964. http://dx.doi.org/10.1096/fj.05-5538fje

Brailoiu, E., D. Churamani, X. Cai, M.G. Schrlau, G.C. Brailoiu, X. Gao, R. Hooper, M.J. Boulware, N.J. Dun, J.S. Marchant, and S. Patel. 2009. Essential requirement for two-pore channel 1 in NAADP-mediated calcium signaling. *J. Cell Biol.* 186:201–209. http://dx.doi.org/10.1083/jcb.200904073

Calcraft, P.J., M. Ruas, Z. Pan, X. Cheng, A. Arredouani, X. Hao, J. Tang, K. Rietdorf, L. Teboul, K.T. Chuang, et al. 2009. NAADP mobilizes calcium from acidic organelles through two-pore channels. *Nature.* 459:596–600. http://dx.doi.org/10.1038/nature08030

Churamani, D., E.A. Carrey, G.D. Dickinson, and S. Patel. 2004. Determination of cellular nicotinic acid-adenine dinucleotide phosphate (NAADP) levels. *Biochem. J.* 380:449–454. http://dx.doi.org/10.1042/BJ20031754

Csanády, L., and B. Törocsik. 2009. Four Ca^{2+} ions activate TRPM2 channels by binding in deep crevices near the pore but intracellularly of the gate. *J. Gen. Physiol.* 133:189–203. http://dx.doi.org/10.1085/jgp.200810109

Fliegert, R., A. Gasser, and A.H. Guse. 2007. Regulation of calcium signalling by adenine-based second messengers. *Biochem. Soc. Trans.* 35:109–114. http://dx.doi.org/10.1042/BST0350109

Fonfria, E., I.C. Marshall, I. Boyfield, S.D. Skaper, J.P. Hughes, D.E. Owen, W. Zhang, B.A. Miller, C.D. Benham, and S. McNulty. 2005. Amyloid beta-peptide(1-42) and hydrogen peroxide-induced toxicity are mediated by TRPM2 in rat primary striatal cultures. *J. Neurochem.* 95:715–723. http://dx.doi.org/10.1111/j.1471-4159.2005.03396.x

Hara, Y., M. Wakamori, M. Ishii, E. Maeno, M. Nishida, T. Yoshida, H. Yamada, S. Shimizu, E. Mori, J. Kudoh, et al. 2002. LTRPC2 Ca^{2+}-permeable channel activated by changes in redox status confers susceptibility to cell death. *Mol. Cell.* 9:163–173. http://dx.doi.org/10.1016/S1097-2765(01)00438-5

Hermosura, M.C., A.M. Cui, R.C. Go, B. Davenport, C.M. Shetler, J.W. Heizer, C. Schmitz, G. Mocz, R.M. Garruto, and A.L. Perraud. 2008. Altered functional properties of a TRPM2 variant in Guamanian ALS and PD. *Proc. Natl. Acad. Sci. USA.* 105:18029–18034. http://dx.doi.org/10.1073/pnas.0808218105

Kaneko, S., S. Kawakami, Y. Hara, M. Wakamori, E. Itoh, T. Minami, Y. Takada, T. Kume, H. Katsuki, Y. Mori, and A. Akaike. 2006. A critical role of TRPM2 in neuronal cell death by hydrogen peroxide. *J. Pharmacol. Sci.* 101:66–76. http://dx.doi.org/10.1254/jphs.FP0060128

Koch-Nolte, F., F. Haag, A.H. Guse, F. Lund, and M. Ziegler. 2009. Emerging roles of NAD^+ and its metabolites in cell signaling. *Sci. Signal.* 2:mr1. http://dx.doi.org/10.1126/scisignal.257mr1

Kolisek, M., A. Beck, A. Fleig, and R. Penner. 2005. Cyclic ADP-ribose and hydrogen peroxide synergize with ADP-ribose in the activation of TRPM2 channels. *Mol. Cell.* 18:61–69. http://dx.doi.org/10.1016/j.molcel.2005.02.033

Lange, I., R. Penner, A. Fleig, and A. Beck. 2008. Synergistic regulation of endogenous TRPM2 channels by adenine dinucleotides in primary human neutrophils. *Cell Calcium.* 44:604–615. http://dx.doi.org/10.1016/j.ceca.2008.05.001

Lin, S., L. Gasmi, Y. Xie, K. Ying, S. Gu, Z. Wang, H. Jin, Y. Chao, C. Wu, Z. Zhou, et al. 2002. Cloning, expression and characterisation of a human Nudix hydrolase specific for adenosine 5′-diphosphoribose (ADP-ribose). *Biochim. Biophys. Acta.* 1594:127–135. http://dx.doi.org/10.1016/S0167-4838(01)00296-5

Malavasi, F., S. Deaglio, A. Funaro, E. Ferrero, A.L. Horenstein, E. Ortolan, T. Vaisitti, and S. Aydin. 2008. Evolution and function of the ADP ribosyl cyclase/CD38 gene family in physiology and pathology. *Physiol. Rev.* 88:841–886. http://dx.doi.org/10.1152/physrev.00035.2007

McHugh, D., R. Flemming, S.Z. Xu, A.L. Perraud, and D.J. Beech. 2003. Critical intracellular Ca^{2+} dependence of transient receptor potential melastatin 2 (TRPM2) cation channel activation. *J. Biol. Chem.* 278:11002–11006. http://dx.doi.org/10.1074/jbc.M210810200

Moreau, C., T. Kirchberger, J.M. Swarbrick, S.J. Bartlett, R. Fliegert, T. Yorgan, A. Bauche, A. Harneit, A.H. Guse, and B.V.L. Potter. 2013. Structure-activity relationship of adenosine 5′-diphosphoribose at the transient receptor potential melastatin 2 (TRPM2) channel: Rational design of antagonists. *J. Med. Chem.* 56:10079–10102. http://dx.doi.org/10.1021/jm401497a

Nagamine, K., J. Kudoh, S. Minoshima, K. Kawasaki, S. Asakawa, F. Ito, and N. Shimizu. 1998. Molecular cloning of a novel putative Ca^{2+} channel protein (TRPC7) highly expressed in brain. *Genomics.* 54:124–131. http://dx.doi.org/10.1006/geno.1998.5551

Olah, M.E., M.F. Jackson, H. Li, Y. Perez, H.S. Sun, S. Kiyonaka, Y. Mori, M. Tymianski, and J.F. MacDonald. 2009. Ca^{2+}-dependent induction of TRPM2 currents in hippocampal neurons. *J. Physiol.* 587:965–979. http://dx.doi.org/10.1113/jphysiol.2008.162289

Perraud, A.L., A. Fleig, C.A. Dunn, L.A. Bagley, P. Launay, C. Schmitz, A.J. Stokes, Q. Zhu, M.J. Bessman, R. Penner, et al. 2001. ADP-ribose gating of the calcium-permeable LTRPC2 channel revealed by Nudix motif homology. *Nature.* 411:595–599. http://dx.doi.org/10.1038/35079100

Perraud, A.L., C. Schmitz, and A.M. Scharenberg. 2003a. TRPM2 Ca^{2+} permeable cation channels: from gene to biological function. *Cell Calcium.* 33:519–531. http://dx.doi.org/10.1016/S0143-4160(03)00057-5

Perraud, A.L., B. Shen, C.A. Dunn, K. Rippe, M.K. Smith, M.J. Bessman, B.L. Stoddard, and A.M. Scharenberg. 2003b. NUDT9, a member of the Nudix hydrolase family, is an evolutionarily conserved mitochondrial ADP-ribose pyrophosphatase. *J. Biol. Chem.* 278:1794–1801. http://dx.doi.org/10.1074/jbc.M205601200

Perraud, A.L., C.L. Takanishi, B. Shen, S. Kang, M.K. Smith, C. Schmitz, H.M. Knowles, D. Ferraris, W. Li, J. Zhang, et al. 2005. Accumulation of free ADP-ribose from mitochondria mediates oxidative stress-induced gating of TRPM2 cation channels. *J. Biol. Chem.* 280:6138–6148. http://dx.doi.org/10.1074/jbc.M411446200

Sano, Y., K. Inamura, A. Miyake, S. Mochizuki, H. Yokoi, H. Matsushime, and K. Furuichi. 2001. Immunocyte Ca^{2+} influx system mediated by LTRPC2. *Science.* 293:1327–1330. http://dx.doi.org/10.1126/science.1062473

Schmid, F., S. Bruhn, K. Weber, H.W. Mittrücker, and A.H. Guse. 2011. CD38: A NAADP degrading enzyme. *FEBS Lett.* 585:3544–3548. http://dx.doi.org/10.1016/j.febslet.2011.10.017

Togashi, K., Y. Hara, T. Tominaga, T. Higashi, Y. Konishi, Y. Mori, and M. Tominaga. 2006. TRPM2 activation by cyclic ADP-ribose at body temperature is involved in insulin secretion. *EMBO J.* 25:1804–1815. http://dx.doi.org/10.1038/sj.emboj.7601083

Tóth, B., and L. Csanády. 2010. Identification of direct and indirect effectors of the transient receptor potential melastatin 2 (TRPM2) cation channel. *J. Biol. Chem.* 285:30091–30102. http://dx.doi.org/10.1074/jbc.M109.066464

Tóth, B., and L. Csanády. 2012. Pore collapse underlies irreversible inactivation of TRPM2 cation channel currents. *Proc. Natl. Acad. Sci. USA.* 109:13440–13445. http://dx.doi.org/10.1073/pnas.1204702109

Tóth, B., I. Iordanov, and L. Csanády. 2014. Putative chanzyme activity of TRPM2 cation channel is unrelated to pore gating. *Proc. Natl.*

Downloaded from http://rupress.org/jgp/article-pdf/145/5/419/1794700/jgp_201511377.pdf by guest on 07 February 2026

Acad. Sci. USA. 111:16949–16954. http://dx.doi.org/10.1073/pnas.1412449111

Uchida, K., K. Dezaki, B. Damdindorj, H. Inada, T. Shiuchi, Y. Mori, T. Yada, Y. Minokoshi, and M. Tominaga. 2011. Lack of TRPM2 impaired insulin secretion and glucose metabolisms in mice. *Diabetes.* 60:119–126. http://dx.doi.org/10.2337/db10-0276

Wang, X., X. Zhang, X.P. Dong, M. Samie, X. Li, X. Cheng, A. Goschka, D. Shen, Y. Zhou, J. Harlow, et al. 2012. TPC proteins are phosphoinositide-activated sodium-selective ion channels in endosomes and lysosomes. *Cell.* 151:372–383. http://dx.doi.org/10.1016/j.cell.2012.08.036

Wehage, E., J. Eisfeld, I. Heiner, E. Jüngling, C. Zitt, and A. Lückhoff. 2002. Activation of the cation channel long transient receptor potential channel 2 (LTRPC2) by hydrogen peroxide. A splice variant reveals a mode of activation independent of ADP-ribose. *J. Biol. Chem.* 277:23150–23156. http://dx.doi.org/10.1074/jbc.M112096200

Yamamoto, S., S. Shimizu, S. Kiyonaka, N. Takahashi, T. Wajima, Y. Hara, T. Negoro, T. Hiroi, Y. Kiuchi, T. Okada, et al. 2008. TRPM2-mediated Ca^{2+}influx induces chemokine production in monocytes that aggravates inflammatory neutrophil infiltration. *Nat. Med.* 14:738–747. http://dx.doi.org/10.1038/nm1758

Downloaded from http://rupress.org/jgp/article-pdf/145/5/419/1794700/jgp_201511377.pdf by guest on 07 February 2026